Superconducting current path and flux line shape in NbTiTa obtained by inter-diffusion process

2008 J. Phys.: Condens. Matter 20 465222

(http://iopscience.iop.org/0953-8984/20/46/465222)

J. Phys.: Condens. Matter **20** (2008) 465222 (6pp) doi:10.1088/0953-8984/20/46/465222

Superconducting current path and flux line shape in NbTiTa obtained by inter-diffusion process

Cristina Bormio-Nunes[1] **and Luis Ghivelder**[2]

[1] Escola de Engenharia de Lorena, Universidade de São Paulo, CP116, Lorena, SP 12602-860, Brazil
[2] Instituto de Física, Universidade Federal do Rio de Janeiro, CP 68528, Rio de Janeiro, RJ 21941-972, Brazil

Received 15 May 2008, in final form 2 October 2008
Published 27 October 2008
Online at stacks.iop.org/JPhysCM/20/465222

Abstract

This investigation presents a comprehensive characterization of magnetic and transport properties of an interesting superconducting wire, Nb–Ti–Ta, obtained through the solid-state diffusion between Nb–12 at.%Ta alloy and pure Ti. The physical properties obtained from magnetic and transport measurements related to the microstructure unambiguously confirmed a previous proposition that the superconducting currents flow in the center of the diffusion layer, which has a steep composition variation. The determination of the critical field also confirmed that the flux line core size is not constant, and in addition it was possible to determine that, in the center of the layer, the flux line core is smaller than at the borders. A possible core shape design is proposed. Among the wires studied, the one that presented the best critical current density was achieved for a diffusion layer with a composition of about Nb–32%Ti–10%Ta, obtained with a heat treatment at 700 °C during 120 h, in agreement with previous studies. It was determined that this wire has the higher upper critical field, indicating that the optimization of the superconducting behavior is related to an intrinsic property of the ternary alloy.

(Some figures in this article are in colour only in the electronic version)

1. Introduction

In terms of applied superconducting properties, the gain in the upper critical field B_{c2} by using Nb–Ti–Ta instead of Nb–Ti can be as high as 2 T at 2 K [1]. In these alloys B_{c2} is controlled by the amount of Ta and the critical current density, J_c, by the volumetric fraction of α-Ti precipitates. However, for the optimization of the critical current density it is observed that, although Ta acts as a weaker β-phase stabilizer than Nb, it is more difficult to obtain α-Ti precipitates in the ternary than in the binary alloys. Some authors focused on the optimization of B_{c2} [1, 2]. Liu *et al* showed that using the proper amounts of Ti and Ta it is possible to get high B_{c2} values, 11.7 T at 4.2 K and 15.4 T at 2 K [1]. Other authors studied the optimization of J_c. The values reported in the literature [3, 4] show $J_c \approx 1600$ A mm^{-2} (10 T). Usually, these Nb–Ti–Ta alloys are produced by electron beam or arc melting, and a great deal of effort must be expended to produce alloys with high homogeneity.

One alternative method of producing the Nb–Ti–Ta superconductor is by combining an Nb–Ta alloy or Nb, Ta with pure Ti, for example using sheets, tubes and bars. The composite is then mechanically processed (extrusion, swaging, drawing) and, after several stacking sequences, the Nb–Ta and Ti are present in small layer thickness. During processing, heat treatments are applied to the composite to form the Nb–Ti–Ta alloy by diffusion, leaving either some Nb–Ta or Ti to compose a second phase material [5]. This kind of material is very untypical since they present a variable composition diffusion layer (DL) that is supposed to be the effective superconducting phase. However, as the composition of the DL changes along the DL length the superconducting properties of the layer are also not constant in this length. Within this scenario, two basic questions arise: does the current flow across the whole DL cross section? How does the flux line look like in this material? We will address these questions in the present study.

A monofilament wire was employed, produced by assembling a Ti rod, a tube of Nb–12 at.%Ta (Nb–12Ta) and a

copper tube. A detailed study of the resulting superconducting properties, such as upper critical field B_{c2}, critical current density J_c, critical temperature T_c and the DL composition profile enabled an understanding of the superconducting current paths and the flux line shape in this superconducting alloy.

It is worth mentioning that the values of J_c obtained in the present work are low when compared to conventional Nb–Ti wires, because the wires under study have superconducting and normal regions in the micrometer scale range. But it is not the aim of this investigation to optimize the wire for technological use, but to study the superconducting properties of this unusual material.

2. Experimental procedure

The experiments were carried out on pieces of the monofilament NbTaTi wires with a final diameter of 0.64 mm with Cu and a nominal diameter of 0.54 mm without Cu, heat treated for 120 h at 700 °C (sample x), 750 °C (sample y) and 800 °C (sample z). The wire transversal section microstructure was observed by scanning electron microscopy (SEM)/backscattered electrons (BSE). The DL concentration profiles of Nb, Ti and Ta were measured from pure Ti to the Nb–12Ta region with energy-dispersive spectroscopy (EDS). The details of the production of this wire were presented elsewhere [6].

Transport measurements of critical current I_c as a function of the magnetic field were carried out in a MaglabExa-Oxford platform, and transport upper critical field B_{c2} and critical temperature T_c measurements were made in a PPMS-QD system. Both these properties were determined by using standard four-wire electrical resistance. In the case of I_c the temperature was fixed at 4.2 K and the field varied up to 5 T. The electrical field criteria used to determine I_c was 1 μV cm^{-1}. The wire samples were placed with the long axis perpendicular to the direction of the applied field. The critical temperature T_c was measured by applying an ac current of 51.7 mA with a frequency of 10 Hz. For the determination of B_{c2}, the current was fixed at 10.4 mA and a frequency of 33 Hz, and the measurements were made at 3.0, 4.2, 5.0, 6.0, 7.0 and 8.0 K. Larger current values were tested in both cases but Joule heating effects were observed. Larger frequencies, up to 1 kHz, did not yield any change on the transport transition values.

The critical temperature was taken as the midpoint of the transition and the upper critical field as the transition onset. The superconducting area of the wires was estimated from SEM electron back-scattering images and corresponds to the diffusion layer transversal area. Magnetic measurements of T_c by ac susceptibility were made in a PPMS-QD system. The magnetic T_c was measured with an ac field of 10 Oe and at a frequency of 10 Hz.

3. Results and discussion

3.1. Microstructure

In figure 1(a) we observe a typical SEM/BSE image of the transversal cross section of sample x. It is possible to identify

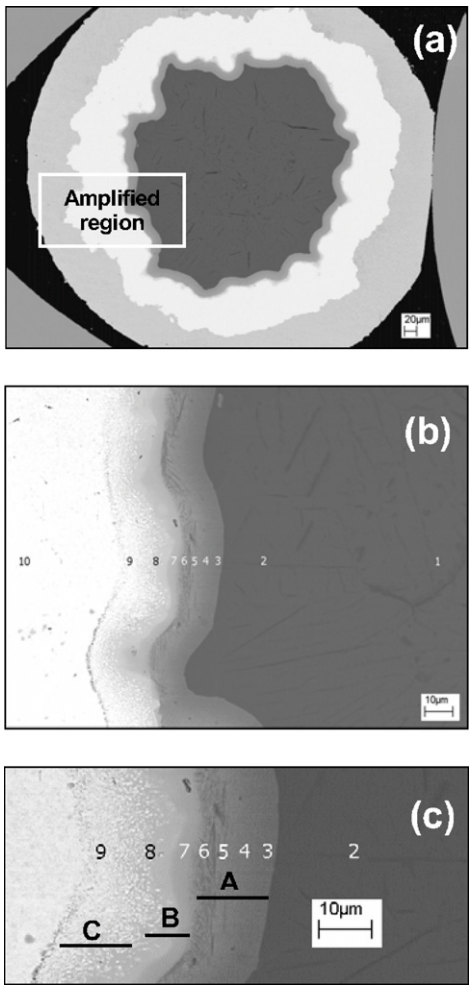

Figure 1. Typical SEM/BSE picture of the Nb–12Ta + Ti wires' transversal section for sample x (HT at 700 °C); (a) whole transversal section, (b) magnification of the indicated region in (a) and (c) higher magnification of the DL, indicating the layer parts A, B and C.

a gray DL between pure Ti (dark gray) and Nb–12Ta (white). Figures 1(b) and (c) are enlargements of the marked region and the numbers 1–10 indicate the points where the EDS measurements were taken. The results of EDS measurements of the Ti, Ta and Nb concentrations are shown in the plots of figures 2(a)–(c). From these measurements and the SEM/BSE pictures the diffusion layer thicknesses are estimated to be 38 and 50 μm for samples x and y, respectively, and greater than 110 μm for sample z. The area of the wire without copper, determined from figure 1 using image analyses, is 0.2376×10^{-6} m^2. The total area for a diameter of 0.64 mm gives an area of 0.3217×10^{-6} m^3, resulting then in a Cu to superconducting area ratio of 1:2.82. For a detailed description of figures 1 and 2 see [6].

3.2. Superconducting properties

AC susceptibility measurements show similar curves of the real χ' and imaginary χ'' components as a function of temperature for all heat treatment (HT) conditions, as shown in figures 3(a) and (b). Both χ' and χ'' curves present two well-defined

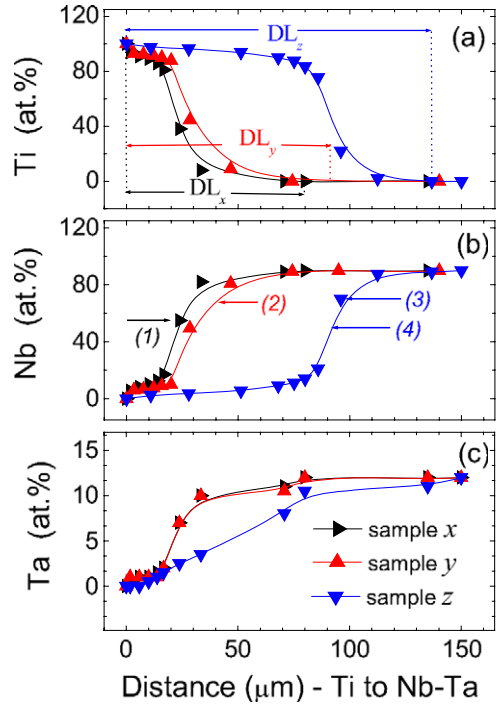

Figure 2. (a) Ti, (b) Nb and (c) Ta concentration (in at.%) profile from the Ti-rich (100%Ti) region to the Nb–12Ta alloy region, measured along the DL length in the transversal section of the wire. The arrows in panel (b) indicate the region of the DL where the supercurrents cross.

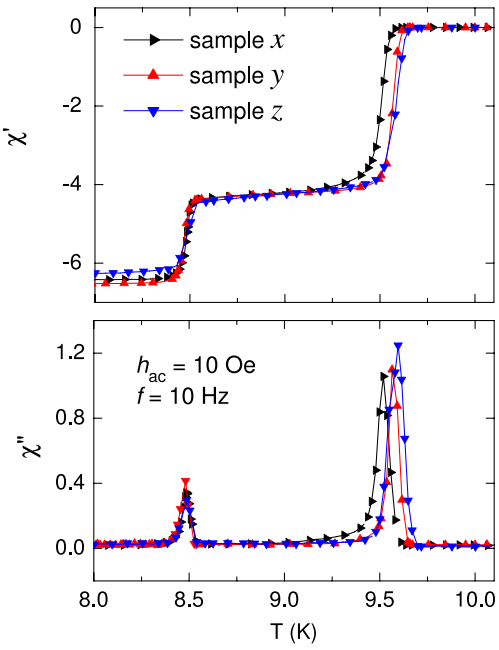

Figure 3. Volume AC susceptibility χ' and χ'' (SI units) of Nb–12Ta+Ti samples x, y and z, heat treated at 700, 750 and 800 °C, respectively, for an ac field of 10 Oe and frequency of 10 Hz.

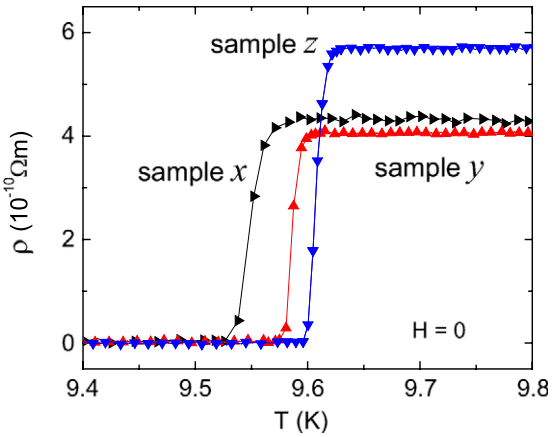

Figure 4. Temperature dependence of the resistivity of Nb–12Ta + Ti samples x, y and z, heat treated at 700, 750 and 800 °C, respectively (zero field).

features. The peaks in χ'' coincide exactly with the middle point of the χ' transitions. The first peak at 8.48 K is consistent with the T_c of Nb–12Ta [7]. The second peak occurs at 9.52, 9.57 and 9.59 K for samples x, y and z, respectively, with an error of about 0.04 K arising from the temperature measurement step. We associate this second transition in T_c to the variable composition diffusion layer. The transition widths are 0.07 K (first transition) and 0.12 K (second transition) for samples x and y, and 0.12 K (first transition) and 0.17 K (second transition) for sample z. The T_c transport measurements curves are shown in figure 4 and these T_c values are very close to those obtained from magnetic measurements, namely 9.52 K (sample x), 9.58 K (sample y) and 9.61 (sample z). The transition width is less than 0.05 K in all cases, with an error of about 0.01 K. The trend in T_c, observed in transport and magnetization measurements, is exactly the same: T_c increases as the HT temperature increases. In relation to the very narrow T_c transition width, one could interpret this as due to a very homogeneous alloy, but this is not the case. In fact, from [8] we find that the values of the measured critical temperature in the ternary alloy are compatible to a very wide range of possible compositions. But if we also measure the B_{c2} on the same samples, it is possible to determine the composition of the DL part that is responsible for these properties, as will be shown in the following.

In figures 5(a)–(c) we present isothermal resistance measurements of the higher critical field B_{c2} for each different HT condition sample. The resistivity was calculated dividing the resistance by distance between the voltage contacts (∼9 mm) and multiplying by the area of the wire without copper (0.2376×10^{-6} m^2). The minimum value of ρ calculated in this way is about 6.0×10^{-10} Ω · m around 3 T. Besides the B_{c2} results, there are two aspects in figure 5 to be highlighted: the observed low normal state resistivity (ρ) and the large magnetoresistance of the wires. In the normal state the low resistivity values come also from the contribution of the copper sheath, estimated, using the Cu to superconductor area ratio 1:2.82, to be 2.1×10^{-10} Ω · m. However, the large normal state magnetoresistance is not understood. The results of the B_{c2} and the transition width ΔB_{c2} are brought together in table 1. As the sample HT temperature increases, B_{c2} decreases and a tendency of the transition broadening is observed as the measurement temperature decreases. In fact,

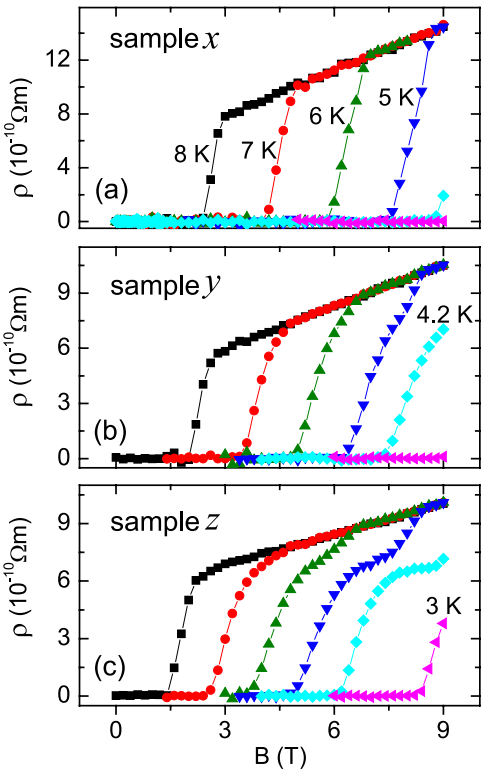

Figure 5. Magnetic field dependence of the resistivity of Nb–12Ta + Ti samples x, y and z, heat treated at 700, 750 and 800 °C, respectively. From left to right, measurements were made at 8, 7, 6, 5, 4.2 and 3 K.

Table 1. Results of upper critical field B_{c2} (at 4.2 K) and transition width ΔB_{c2}, at measurement temperatures of 3, 4.2, 5, 6, 7 and 8 K.

	Sample x		Sample y		Sample z	
T (K)	B_{c2} (T)	ΔB_{c2} (T)	B_{c2} (T)	ΔB_{c2} (T)	B_{c2} (T)	ΔB_{c2} (T)
3	—	—	9.00	—	8.30	—
4.2	8.65	—	7.35[a]	(>2)	6.08	<3
5	7.33	1.49	6.27	2.16	4.77[a]	3.23
6	5.73	1.23	4.90	1.79	3.58[a]	3.03
7	3.97	1.01	3.41	1.37	2.48	2.32
8	2.26	0.74	1.98	0.86	1.40	1.17

[a] Double transition tendency.

from figure 5(c) (sample z) this broadening develops to the split of one transition into two transitions at 5 K.

In figure 6, the Nb–Ti–Ta Gibbs triangle [10] is presented with iso-B_{c2} (figure 6(a)) and iso-T_c (figure 6(b)) lines taken from [8]. Based on the results of T_c and B_{c2} at 4.2 K we found four points in this Gibbs triangle (1, 2, 3 and 4) defined by the pairs (T_c, B_{c2}). It was then possible to estimate the composition of the part of the DL that is reflecting the properties of each one of the four pairs. It is reasonable to conclude that the supercurrents in these transport measurements are flowing in the region of the layer that has the best superconducting properties.

In table 2 we list the values of B_{c2} measured at 4.2 K and T_c, together with the likely values of composition of the DL part, which are responsible for the best superconducting

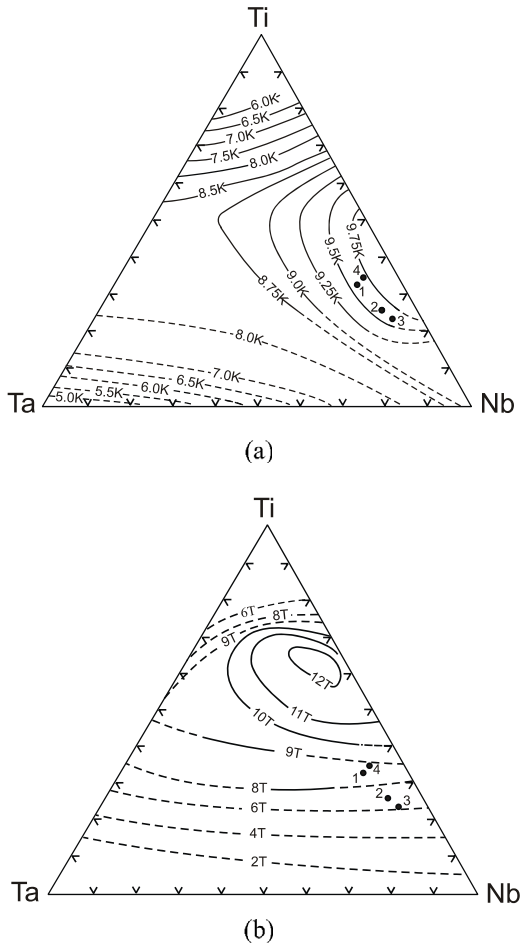

Figure 6. Gibbs triangles of the system Nb–Ta–Ti showing: (a) iso-T_c and (b) iso-B_{c2} lines (4.2 K) [8]. Points 1, 2 and 3 indicate the compositions of the alloys determined for each sample using T_c and B_{c2} experimental values (table 2).

Table 2. Superconducting properties of samples x, y and z and the related composition of the DL part: x (HT at 700 °C), y (HT at 750 °C) and z (HT at 800 °C).

Sample	HTT (K)	B_{c2} (4.2 K)	T_c (K)	Estimated composition (at.%)	Points in figures 2 and 6
x	973	8.65	9.52	Nb–32%Ti–10%Ta	1
y	1023	7.30	9.55	Nb–25%Ti–8%Ta	2
z	1073	6.10	9.61	Nb–25%Ti–5%Ta	3
		8.90		Nb–35%Ti–8%Ta	4

properties. Further inspection of figure 2 shows that this composition of each sample is localized just around the DL center part and in this place the DL has a steep composition variation. These regions are indicated in figure 2(b) by points 1–4 in the experimental composition profile curves. For all three samples these alloy compositions are in the Nb-rich regions and located in part B of the DL as shown in figure 1(c). For the wire obtained in the present work, the best value of B_{c2} obtained is that of the ternary alloy with composition 58Nb–32Ti–10Ta (in at.%). However, to get the best compromise between T_c and B_{c2} one should choose the composition of

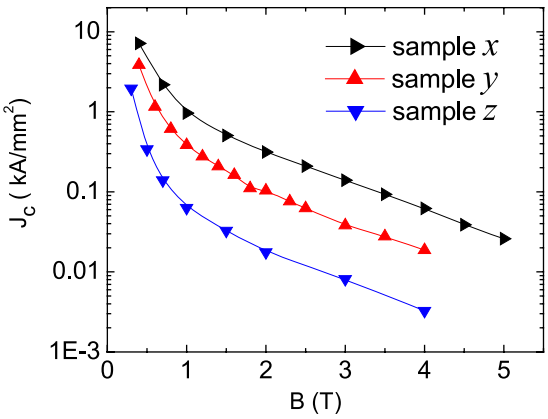

Figure 7. Magnetic field dependence of the J_c versus magnetic field of Nb12Ta+Ti samples x, y and z : x (HT at 700 °C), y (HT at 750 °C) and z (HT at 800 °C).

65Nb–33Ti–1.5Ta (Nb–21 wt%Ti–4 wt%Ta) with $T_c \approx 9.3$ K and $B_{c2} \cong 12$ T at 4.2 K [8].

The results of critical current density J_c for the three samples studied are shown in figure 7. J_c was calculated by dividing the critical current I_c by the area of the ring formed by the DL in the transversal section of the wire. The shapes of the DL frontiers were approximated to circles. The areas are 0.0258 mm, 0.0289 mm^2 and 0.0613 mm^2 for samples x, y and z, respectively. It is clear that the sample HT temperature increase is detrimental to J_c, despite the increase of ternary phase volume (DL size). In fact, for the largest DL (sample z, HT at 800 °C), 70% of its length is very rich in Ti (95.6 at.%) and has an almost constant composition. Therefore this part of the DL has very low T_c and B_{c2} values [8] and ineffective superconducting properties. In contrast, there is noted a tendency of an increase of J_c for higher fields in the sample HT at the lowest temperature. We conclude then that this improvement in J_c (figure 7) is due to the sharp part of the DL [9, 11] because as the DL sharpness increases (sample $z \rightarrow y \rightarrow x$) there is a corresponding ΔB_{c2} decrease (table 1).

Based on the T_c, B_{c2} and J_c results, the optimization of the superconducting properties of this kind of wire, in order to get a wire with good B_{c2} and T_c, simultaneously should have a very low Ta content (≈1–2%) and Nb around 61% (atomic) and for a high J_c a sharp DL composition profile. We suggest that by lowering the HT temperature below 700 °C for longer periods this could be achieved, because the coefficient of inter-diffusion between Ta and α-Ti is smaller as the temperature is reduced [6]. This condition will prevent the excessive growth of the DL and thus a sharp composition profile should develop.

Concerning the flux line in this kind of material, it is natural to think that, due to the variation of the DL composition and therefore the change in B_{c2}, along the DL extent, the flux line core diameter must change, since the core diameter ξ is a function of the upper critical field, $\xi = [\phi_0/2\pi B_{c2}]^{1/2}$. The core diameter is smallest where B_{c2} is the largest and the supercurrents flow at this point because of the highest free superconducting phase volume (not normal as the core). Looking at the transverse section of the wire in figure 1, the

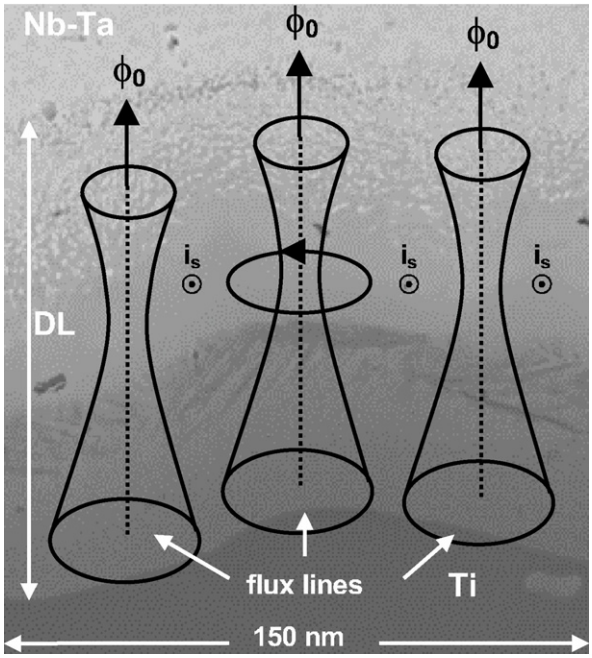

Figure 8. Sketch of the flux lines in the transverse section of the Nb–12Ta + Ti wire for the field applied perpendicular to the wire axis. Closest to Nb–Ta and Ti, the DL has lower B_{c2} and therefore the FL core (ξ) is larger than at the DL central part that has higher B_{c2} values and then smaller cores ($\xi = [\phi_0/2\pi B_{c2}]^{1/2}$). Supercurrents ($i_s$) flow close to the DL central part because there the core is smaller and consequently the superconducting region has higher volume.

flux line core crossing the DL from region C (close to Nb–Ta) to region A (close to pure Ti) have a larger diameter in these regions (lower B_{c2}). This core diameter shrinks in the DL center region, reaching a minimum value in region B (higher B_{c2}). For example, consider samples x and y at 4.2 K. For both wires at the ends of the DL, the composition in region C is about 70Nb–23Ti–7Ta and in region A is about 92Ti–8Nb. By taking the B_{c2} values from [8] (figure 6), region C has a core diameter of about 7.4 nm ($B_{c2} \cong 6$ T) and region A of about 18.1 nm ($B_{c2} \cong 1$ T $\ll 6$ T). In region B, the core diameter is minimum and is calculated from B_{c2} values to be 6.2 nm in sample x and 6.7 nm in sample y. Therefore, based on this previous discussion, in figure 8 we sketch the structure of a flux line core crossing the DL from region C to A, for a field applied perpendicular to the wire axis.

4. Conclusions

In the present investigation, it was unambiguously determined by direct experimental evidence that, in materials produced by solid-state inter-diffusion between Ti and Nb–Ta (Nb), the supercurrents flow in a relatively small fraction of the DL, which presents a sharp composition variation and improved upper critical field, B_{c2}. This was suggested by indirect evidence in a previous study [11].

The results show that the flux line cores must have a peculiar shape in this kind of material; a smaller size in the center of the diffusion layer compared to the sizes at the borders of the layer. This finding showed that the models to

explain flux pinning in the commercial Nb–Ti superconductors should be re-evaluated, because the already identified presence of composition gradients around the α-Ti precipitates (pinning centers) [12] certainly also cause a variation of the core diameter in this material.

Acknowledgments

This work was partially supported by the Brazilian agencies Fapesp, Faperj and CNPq.

References

[1] Liu H, Gregory E, Faase K J and Warnes W H 1996 *Adv. Cryog. Eng.* **42** 1135–42
[2] Shimada T *et al* 1999 *IEEE Trans. Appl. Supercond.* **9** 1731–4
[3] Verdenikov G P *et al* 2000 *IEEE Trans. Appl. Supercond.* **10** 1038–41
[4] Chernyi O V *et al* 2001 *IEEE Trans. Appl. Supercond.* **11** 3796–9
[5] Rudziak M K, Seutjeuns J M, Wong T and Wong J 1996 *Adv. Cryog. Eng.* **42** 1127–33
[6] Bormio-Nunes C, Gomes P M N, Tirelli M A and Ghivelder L 2005 *J. Appl. Phys.* **98** 043907
[7] Rapp Ö and Pokorny M 1972 *Phys. Scr.* **6** 200–5
[8] Suenaga M and Ralls K M 1969 Some superconducting properties of Ti–Nb–Ta alloys *J. Appl. Phys.* **40** 4457–3
[9] Bormio-Nunes C, Sandim M J R, Edwards E R and Ghivelder L 2006 *Supercond. Sci. Technol.* **19** 1063–7
[10] West D R F 1982 *Ternary Equilibrium Diagrams* (New York: Chapman and Hall)
[11] Bormio-Nunes C, Sandim M J R and Ghivelder L 2007 *J. Phys.: Condens. Matter* **19** 446204
[12] Lazarev B G, Ksenofontov V A, Mikkailovskii I M and Velikodnaya O A 1998 *Low Temp. Phys.* **24** 205